JOURNAL OF MAGNETIC RESONANCE **133,** 364–367 (1998)
ARTICLE NO. MN981492

An α/β-HSQC-α/β Experiment for Spin-State Selective Editing of IS Cross Peaks

Patrik Andersson,* Arto Annila,† and Gottfried Otting*,[1]

*Department of Medical Biochemistry and Biophysics, Karolinska Institute, S-171 77 Stockholm, Sweden; and †VTT Chemical Technology, FIN-02044 Espoo, Finland

Received February 19, 1998; revised April 23, 1998

A generalized version of the TROSY experiment allows the spin-state selective editing of the four multiplet components of ^{15}N–^{1}H cross peaks of amide groups in proteins into four different subspectra, with no penalty in sensitivity. An improvement by $\sqrt{2}$ in sensitivity results, if only two of the four multiplet components are selected. Use of the experiment for the measurement of $^{1}J_{HN}$ coupling constants is discussed. A water flip-back version of the experiment is demonstrated with a 45 kDa fragment of ^{15}N/^{2}H labeled *Staphylococcus aureus* **gyrase B.** © 1998 Academic Press

Key Words: **one-bond coupling constants;** *Staphylococcus aureus* **gyrase B; TROSY; α/β-HSQC-α/β; spin-state selective editing.**

Spin-state selective editing allows the separation of individual multiplet components into different subspectra, facilitating the measurement of the corresponding coupling constants (*1–5*). Furthermore, cross correlation between dipole–dipole and CSA relaxation affects different multiplet components differently, so that, in some subspectra, signal heights and resolution can be better than in a corresponding spectrum recorded with heteronuclear decoupling (*6*). For doublet components separated by heteronuclear one-bond coupling constants, spin-state selective editing can readily be achieved by experiments using exclusively nonselective pulses (*1–10*). This Communication presents a generalized version of the TROSY (*t*ransverse *r*elaxation *o*ptimized *s*pectroscop*y*) experiment (*6*).[2] Like HSQC experiments recorded with double α/β-half-filter (*5*), the new, generalized TROSY scheme allows the editing of all four multiplet components of an HSQC cross peak between spins I and S, recorded without heteronuclear decoupling, can be separated into different subspectra. The generalized TROSY experiment, henceforth referred to as an α/β-HSQC-α/β experiment, provides superior sensitivity.

Figure 1 shows the pulse sequence of the generalized TROSY experiment discussed here. The main differences from the original TROSY pulse sequence are the omission of a pulsed field gradient (PFG) after the second 90°(^{1}H) pulse and the storage of different FIDs into different data sets. In the original TROSY experiments, the PFG serves for the suppression of the water resonance and of residual magnetization which is in-phase with respect to the heteronucleus. In the new pulse scheme, bipolar gradients during the evolution time t_1 prevent radiation damping of the water magnetization (*11*). The water magnetization is flipped back to the positive *z*-axis by the last 90°(^{1}H) pulse, avoiding its saturation and the transfer of saturation from the water to the protein (*12, 13*). Residual in-phase magnetization present after the initial delay 2τ is purged by cycling the phase ϕ_2 in two steps.

For analysis of the pulse sequence, we use the product operator formalism with Cartesian operators (*14*), omitting signs and normalization factors. For a two-spin system with the operators H and N representing the spins of an amide proton and amide nitrogen, respectively, the term H_zN_x is present at the start of the evolution time t_1. At the end of the evolution time, this term has evolved into the four terms listed in Table 1. Table 1 shows the fate of each of these until the start of the detection period t_2. Remarkably, all four terms result in observable magnetization. They represent all possible combinations of in-phase and antiphase multiplicity: term I leads to a cross peak which is in-phase in the F_1 and F_2 frequency dimensions, term II to a cross peak which is in-phase in F_1 and antiphase in F_2, term III to a cross peak which is antiphase in F_1 and in-phase in F_2, and term IV to a doubly antiphase cross peak. If all terms were absorptive in both dimensions, their sum would result in a single component of the ^{15}N–^{1}H cross peak multiplet. Since the signals from terms I and IV are dispersive in both dimensions, when the signals from terms II and III are phased to be absorptive, these two pairs of terms must be separated and phase corrected before summation. The terms I and II change their sign with the sign of the phase ϕ_4, and the terms II and IV change their sign when ϕ_5 is phase alternated. Therefore, summation and subtraction of two data sets A and B, recorded with $\phi_4 = y$, $\phi_5 = x$, and with $\phi_4 = -y$, $\phi_5 = -x$, respectively, separates the terms II and III from the terms I and IV. Subsequent phase correction of the difference data set A − B by 90° in both dimensions and additive or subtractive combination with the sum data set A + B yields two subspectra

[1] To whom correspondence should be addressed.

[2] The generalized TROSY scheme was presented at the Symposium on Peptide–Protein Interactions, 13–14 February, 1998 in Helsinki, Finland.

1090-7807/98 $25.00

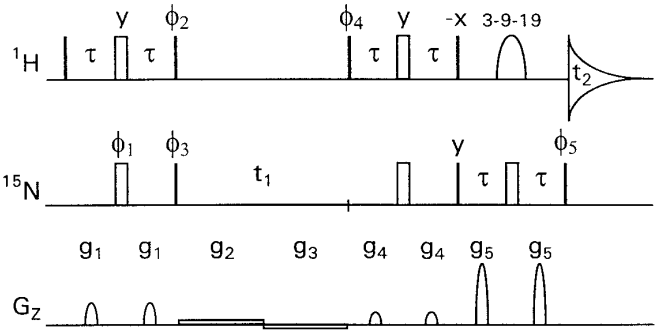

FIG. 1. Generalized TROSY pulse sequence for spin-state selective, subspectral editing of ^{15}N–^{1}H cross peaks. $\tau = 1/(4\ ^1J_{HN})$. Narrow (wide) bars represent 90° (180°) flip angle pulses. The bell shape represents a 3–9–19 pulse (*17*), selectively refocusing the amide protons. All rectangular pulses, except where noted, are applied with phase *x*. Phase cycle: $\phi_1 = x$; $\phi_2 = y, y, -y, -y$; $\phi_3 = y, -y$; receiver $= x, -x, -x, x$. For subspectral editing, four data sets A to D are recorded, with (A) $\phi_4 = y$, $\phi_5 = x$; (B) $\phi_4 = -y$, $\phi_5 = -x$; (C) $\phi_4 = -y$, $\phi_5 = x$; (D) $\phi_4 = y$, $\phi_5 = -x$, and recombined as described in Table 2. Quadrature detection in the indirect frequency dimension is achieved by simultaneously incrementing the phases ϕ_1 and ϕ_3 with each increment of the evolution time t_1. The ^{1}H carrier is set at the water resonance for water flip-back. Pulsed field gradients were applied with a sine-bell shape and a duration of 500 μs, except for the bipolar gradients during t_1, which were rectangular and increasing in duration with t_1 (*11*). Gradient strengths: $g_{1,2,3,4,5} = 2.5, 0.5, -0.5, 1.5, 7.0$ G/cm.

with a single multiplet component for each cross peak. Similarly, two data sets can be recorded with $\phi_4 = -y$, $\phi_5 = x$, and with $\phi_4 = y$, $\phi_5 = -x$, respectively, to obtain the other two subspectra in a completely analogous way (Table 2).

Subspectral editing in the way described here improves the sensitivity by $\sqrt{2}$ over the original TROSY experiment, where half of the signal intensity present in the FIDs is removed by phase cycling (*6*). Furthermore, a second subspectrum containing another component of each cross peak multiplet is obtained from the same data which can be used to measure the $^1J_{HN}$ coupling constant. If effects from relaxation and long-range couplings can be neglected, the sensitivity of the modified experiment is half that of an HSQC spectrum recorded with decoupling in both dimensions and sensitivity enhancement (*15, 16*).

For experimental verification, spectra were recorded with a ^{15}N/^{2}H labeled domain of *Staphylococcus aureus* gyrase B, which has a molecular weight of 45 kDa for the unlabeled protein and a rotational correlation time of 23 ns (*13*). Figure 2A shows an overview of the ^{15}N–^{1}H correlations observed in the β-HSQC-β subspectrum. This multiplet component is narrowed in both dimensions by cross correlation between dipole–dipole and CSA relaxation (*6*). Figures 2B to E show a comparison of cross-sections through the β-HSQC-β (Fig. 2B) and β-HSQC-α (Fig. 2C) subspectra, recorded with the pulse sequence of Fig. 1, with the corresponding cross-sections through a spectrum recorded with the same pulse sequence, but using the original TROSY phase cycle (*6*) (Fig. 2D) and through a conventional FHSQC spectrum recorded with heteronuclear decoupling in both frequency dimensions (*13*) (Fig. 2E). As expected, the new editing scheme yields the β-HSQC-β subspectrum with the same signal-to-noise ratio as the original TROSY experiment, but in half the time (Fig. 2B and C). The cross peak intensities in the β-HSQC-β subspectrum are, however, on average 15% lower than those observed in a conventional, decoupled FHSQC spectrum recorded without sensitivity enhancement (Fig. 2B and E). Figure 3 shows the four multiplet components of a representative ^{15}N–^{1}H cross peak from the four different subspectra recorded with the scheme of Fig. 1 and Table 2. On average, the peak intensities do not vary more than twofold between the different subspectra. Neglecting relaxation, a sensitivity advantage by $\sqrt{2}$ would be predicted for the FHSQC compared to the β-HSQC-β spectrum. In addition, transverse relaxation during the additional delay 2τ (Fig. 1) causes the loss of about $1/\sqrt{2}$ of the magnetization in the β-HSQC-β spectrum, as the average relaxation time of N_xH_x terms in the gyrase domain is about 21 ms (*13*). While the cross correlation effects at 600 MHz ^{1}H frequency were thus not sufficient to raise the signal heights in the

TABLE 1

Product Operators Present after Different Points of the Pulse Sequence of Fig. 1 following the Evolution Time t_1[a]

	Time points					
Term no.	t_1	$90°_y$(H)	2τ	$90°_x$(H), $90°_y$(N)	2τ	$90°_x$(N)
I	$H_zN_x\cos(\Omega t_1)\cos(\pi J t_1)$[b]	H_xN_x	H_xN_x	H_xN_z	H_y	H_y[c]
II	$H_zN_y\sin(\Omega t_1)\cos(\pi J t_1)$	H_xN_y	H_xN_y	H_xN_y	H_xN_y	H_xN_z[d]
III	$N_y\cos(\Omega t_1)\sin(\pi J t_1)$	N_y	H_zN_x	H_yN_z	H_x	H_x[e]
IV	$N_x\sin(\Omega t_1)\sin(\pi J t_1)$	N_x	H_zN_y	H_yN_y	H_yN_y	H_yN_z[c]

[a] For $\tau = 1/(4J)$.
[b] Trigonometric factors are shown only in this column.
[c] Depends on τ with $\sin(\pi J 2\tau)$.
[d] Independent of τ.
[e] Depends on τ with $\sin^2(\pi J 2\tau)$.

TABLE 2
Linear Combinations Yielding the Four Different Subspectra

Subspectrum	^{15}N–^{1}H cross peak multiplet components[a]	Linear combinations[b]
β-HSQC-β	x x x •	a = A + B, b = A − B, a + b_{90}
α-HSQC-α	• x x x	a = A + B, b = A − B, a − b_{90}
α-HSQC-β	x • x x	c = C + D, d = C − D, c + d_{90}
β-HSQC-α	x x • x	c = C + D, d = C − D, c − d_{90}

[a] Only the filled multiplet component is observed; crosses identify the location of absent multiplet components. The top right component of the cross peak multiplet is assumed to be high-field (most shielded) in both frequency dimensions (*18*).

[b] The data sets A–D are recorded with $\phi_{4,5} = y, x$ (A); $-y, -x$ (B); $-y, x$ (C); $y, -x$ (D) (Fig. 1). The subscript '90' denotes a 90° phase correction of the respective data set in both dimensions which can be achieved in the time domain, e.g., by exchanging the real and imaginary part of each complex data point and taking the complex conjugate.

β-HSQC-β spectrum above those observed in the decoupled FHSQC spectrum, a β-HSQC-β spectrum recorded at 800 MHz under otherwise identical conditions showed on average 1.1 ± 0.3 times higher signals than the corresponding decoupled FHSQC spectrum, and 3.4 ± 1.0 higher signals than the α-HSQC-α spectrum.

For measurements of $^{1}J_{HC}$ couplings, the narrowest multiplet components are those which are low-field in the ^{13}C dimension (*5*). Four data sets must be recorded, however, to obtain two subspectra at the same F_1 chemical shift with the scheme of Fig. 1 (Table 2). Such a protocol still yields spectra with twofold better sensitivity than the use of a double α/β-half-filter (*5*), although the sensitivity gap could be reduced by the use of a double α/β-half-filter with shorter filter delays. The α/β-HSQC-α/β experiment of Fig. 1 would be expected to generate more crosstalk between the different subspectra, when the delay τ does not perfectly match 1/(4*J*), since the magnitude of the different terms depends differently on τ (Table 1). Crosstalk would further be expected from different relaxation rates of the terms shown in Table 1, although crosstalk was experimentally found to be unimportant in our ^{15}N–^{1}H experiments. The most important limitation for measurement of one-bond coupling constants by the α/β-HSQC-α/β experiment may be small phase instabilities arising from the fact that the last 90°(^{1}H) pulse cannot be phase cycled without compromising the sensitivity enhancement scheme. Finally, the pulse sequence of Fig. 1 reduces the information content as it suppresses the ^{15}N–^{1}H cross peaks from NH_2 and NH_3 groups. On the other hand, this effect is beneficial for the measurement of $^{1}J_{HN}$ couplings from cross peaks of backbone amide groups

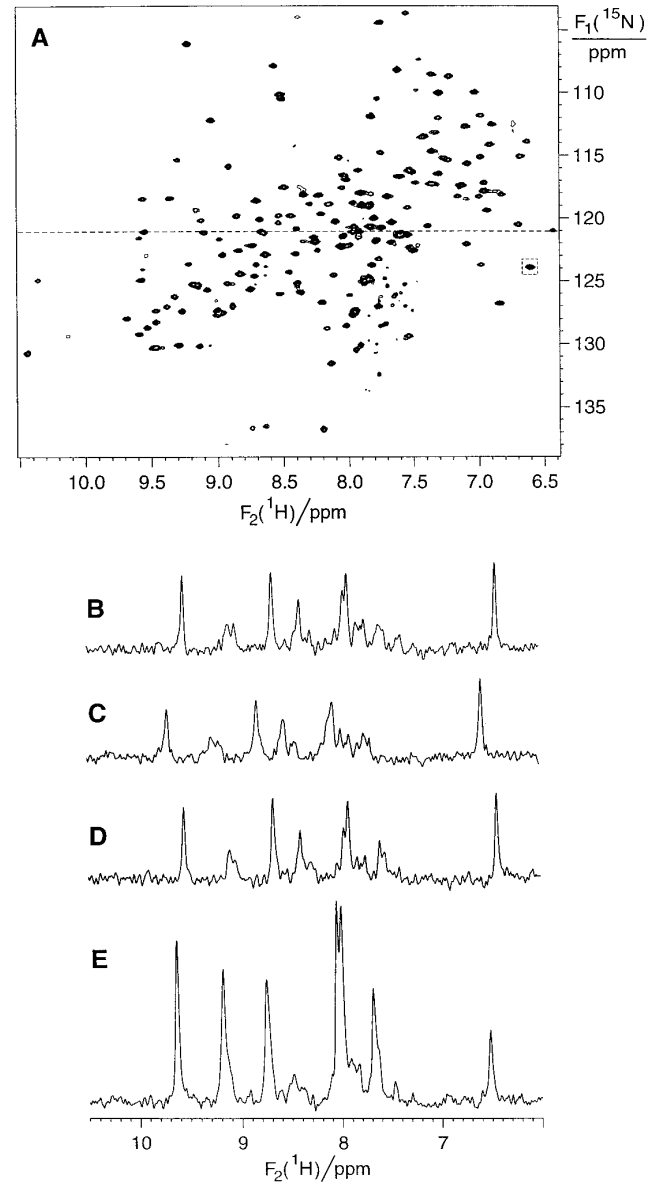

FIG. 2. ^{15}N–^{1}H correlation spectra of a 0.7 mM solution of uniformly ^{15}N-labeled and deuterated (>95%) sample of the N-terminal fragment of *Staphylococcus aureus* gyrase B (residues 1–405), recorded at pH 8.6 and 25°C on a Bruker DMX 600 NMR spectrometer. Experimental parameters: ^{1}H frequency = 600 MHz, τ = 2.78 ms, t_{1max} = 41 ms, t_{2max} = 102 ms. (A) Overview over the β-HSQC-β subspectrum recorded with the pulse sequence of Fig. 1. Total recording time 3 h. The dashed line identifies the location of the cross-section shown in (B). The box identifies the cross peak shown in Fig. 3. (B) Cross-section through the β-HSQC-β subspectrum of (A). (C) Corresponding cross-section through a β-HSQC-α subspectrum recorded with the same parameters. (D) Cross-section through a spectrum recorded with the pulse sequence of Fig. 1 in 6 h, using the original TROSY phase cycle (*6*). (E) Cross-section through a FHSQC spectrum recorded with heteronuclear decoupling in both dimensions in 3 h (*13*). The cross-section were chosen to show the maximum peak height for the cross peak at 8.75 ppm. The cross-sections shown in (B)–(D) were plotted on the same absolute scale, whereas the cross-section in (E) was scaled by $\sqrt{2}$ to obtain the same level of white noise.

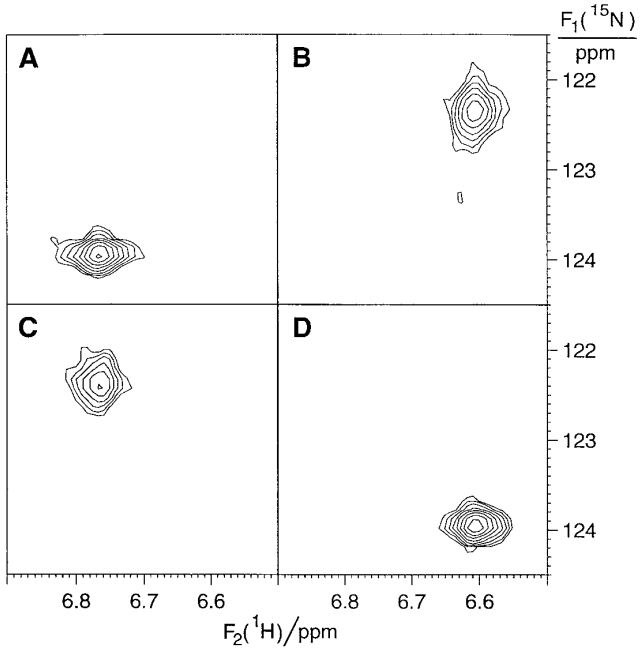

FIG. 3. Multiplet components of the ^{15}N–^{1}H cross peak identified in Fig. 2A, observed in β-HSQC-α (A), α-HSQC-β (B), α-HSQC-α (C), and β-HSQC-β (D) subspectra recorded with the pulse sequence of Fig. 1. The pairs of β-HSQC-α/α-HSQC-β and α-HSQC-α/β-HSQC-β subspectra were obtained from four data sets recorded with a total experimental time of 6 h (Table 2). Contour levels were plotted on an exponential scale, where each level is $\sqrt{2}$ higher than the preceding one.

which overlap with those from side chain NH_2 groups in a conventional HSQC spectrum.

ACKNOWLEDGMENTS

Encouragement and support by Dr. Hans Senn (Hoffmann-La Roche, Basel), financial support from the Swedish Natural Science Research Council (project 10161), and access to the 800 MHz NMR spectrometer at the European large scale facility for biomolecular NMR at the University of Frankfurt are gratefully acknowledged. P.A. acknowledges an SSF fellowship within the Strategic Research in Structural Biology program.

REFERENCES

1. A. Meissner, J. Ø. Duus and O. W. Sørensen, Spin-state selective excitation. Application for E.COSY-type measurement of J_{HH} coupling constants, *J. Magn. Reson.* **128,** 92–97 (1997).
2. A. Meissner, J. Ø. Duus, and O. W. Sørensen, Integration of spin-state-selective excitation into 2D NMR correlation experiments with heteronuclear ZQ/2Q π rotations for $^{1}J_{XH}$-resolved E.COSY-type measurement of heteronuclear coupling constants in proteins, *J. Biomol. NMR* **10,** 89–94 (1997).
3. M. D. Sørensen, A. Meissner and O. W. Sørensen, Spin-state-selective coherence transfer via intermediate states of two-spin coherence in IS spin systems: application to E.COSY-type measurement of J coupling constants, *J. Biomol. NMR* **10,** 181–186 (1997).
4. P. Andersson, K. Nordstrand, M. Sunnerhagen, E. Liepinsh, I. Turovskis, and G. Otting, Heteronuclear correlation experiments for the determination of one-bond coupling constants, *J. Biomol. NMR,* in press.
5. P. Andersson, J. Weigelt, and G. Otting, Spin-state selection filters for the measurement of heteronuclear one-bond coupling constants, *J. Biomol. NMR,* in press.
6. K. Pervushin, R. Riek, G. Wider, and K. Wüthrich, Attenuated T_2 relaxation by mutual concellation of dipole–dipole coupling and chemical shift anisotropy indicates an avenue to NMR structures of very large biological macromolecules in solution, *Proc. Natl. Acad. Sci. USA* **94,** 12366–12371 (1997).
7. N. C. Nielsen, H. Thøgersen, and O. W. Sørensen, A systematic strategy for design of optimum coherent experiments applied to efficient interconversion of double- and single-quantum coherences in nuclear magnetic resonance, *J. Chem. Phys.* **105,** 3962–3968 (1996).
8. N. C. Nielsen, H. Thøgersen, and O. W. Sørensen, Doubling the sensitivity of INADEQUATE for tracing out the carbon skeleton of molecules by NMR, *J. Am. Chem. Soc.* **117,** 11365–11366 (1996).
9. A. Ross, M. Czisch, and T. A. Holak, Selection of simultaneous coherence pathways with gradient pulses, *J. Magn. Reson.* **A118,** 221–226 (1996).
10. M. Sattler, J. Schleucher, O. Schedletzky, S. J. Glaser, C. Griesinger, N. C. Nielsen, and O. W. Sørensen, α&β HSQC, an HSQC-type experiment with improved resolution for I_2S groups, *J. Magn. Reson.* **A119,** 171–179 (1996).
11. V. Sklenář, Suppression of radiation damping in multidimensional NMR experiments using magnetic field gradients, *J. Magn. Reson.* **A114,** 132–135 (1995).
12. S. Mori, C. Abeygunawardana, M. O. Johnson, and P. S. M. van Zijl, Improved sensitivity of HSQC spectra of exchanging protons at short interscan delays using a new fast HSQC (FHSQC) detection scheme that avoids water saturation, *J. Magn. Reson.* **B108,** 94–98 (1995).
13. P. Andersson, B. Gsell, B. Wipf, H. Senn, and G. Otting, HMQC and HSQC experiments with water flip-back optimized for large proteins, *J. Biomol. NMR,* in press.
14. O. W. Sørensen, G. W. Eich, M. H. Levitt, G. Bodenhausen, and R. R. Ernst, Product operator formalism for the description of NMR pulse experiments, *Prog. NMR Spectr.* **16,** 163–192 (1983).
15. J. Cavanagh, A. G. Palmer III, P. E. Wright, and M. Rance, Sensitivity improvement in proton-detected two-dimensional heteronuclear relay spectroscopy, *J. Magn. Reson.* **91,** 429–436 (1991).
16. A. G. Palmer III, J. Cavanagh, P. E. Wright and M. Rance, Sensitivity improvement in proton-detected two-dimensional heteronuclear correlation NMR spectroscopy, *J. Magn. Reson.* **93,** 151–170 (1991).
17. V. Sklenář, M. Piotto, R. Leppik, and V. Saudek, Gradient-tailored water suppression for ^{1}H–^{15}N HSQC experiments optimized to retain full sensitivity, *J. Magn. Reson.* **A109,** 246–249 (1994).
18. M. H. Levitt, The signs of frequencies and phases, *J. Magn. Reson.* **126,** 164–182 (1997).